Dual-Band and Polarization-Flexible Cavity Antenna Based on Substrate Integrated Waveguide

Hanseung Lee, *Student Member, IEEE*, Youngje Sung, Chung-Tse Michael Wu, *Member, IEEE*, and Tatsuo Itoh, *Life Fellow, IEEE*

***Abstract*—In this letter, a novel dual-band and polarization-flexible substrate integrated waveguide (SIW) cavity antenna is proposed. The SIW cavity used for the antenna is excited by a conventional TE_{120} mode for its first resonance. With the intervention of the slot, a second resonance excited by a modified-TE_{120} mode is also generated, thereby providing a broadside radiation pattern at two resonant frequencies. In addition, the proposed antenna has two orthogonal feeding lines. Therefore, it is possible to provide any six major polarization states. In this letter, three major polarization cases are simulated and compared to measured results. Since modern communication systems require multifunctional antennas, the proposed antenna concept is a promising candidate.**

***Index Terms*—Dual-band, polarization, slot antennas, substrate integrated waveguide.**

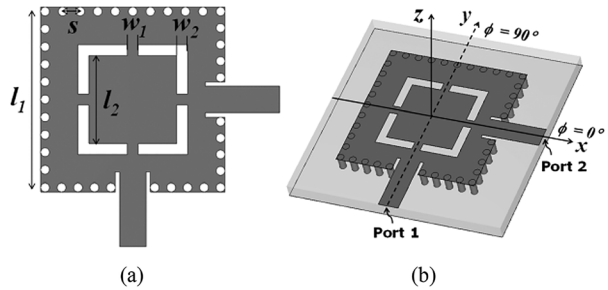

Fig. 1. (a) Proposed antenna top view and (b) perspective view. (Parameters: $l_1 = 16.8$ mm, $l_2 = 8$ mm, $w_1 = 1$ mm, $w_2 = 1$ mm, $s = 1.6$ mm.).

I. Introduction

MANY modern communication systems demand multifunctional antennas equipped with multiband characteristic or polarization flexibility. For example, mobile devices with compact size prefer using single multiband antennas instead of multiple antennas with different bands [1]. Satellite links are generally sustained with multiple frequency bands. Therefore, antennas with multiband characteristics are required [2]. An antenna equipped with polarization flexibility helps to increase channel capacity and enhance receiving power by mitigating multipath fading effects [3] and [4]. Moreover, a polarization-flexible antenna can be beneficial in satellite communication systems in which it is difficult to align between antennas. Under these circumstances, microstrip-line-based antennas with both multiband capability and polarization flexibility have been proposed [5], [6].

In this letter, a dual-band and polarization-flexible antenna is implemented with a substrate integrated waveguide (SIW) cavity structure. An SIW cavity structure as an antenna resonator is promising because the fabrication is simple and the structure has a high power-handling capability. In an array configuration, an SIW cavity is also able to mitigate couplings between radiating elements. These features have been utilized in designing the proposed antenna. The proposed SIW cavity antenna creates broadside radiation patterns similar to a patch antenna at two targeted frequencies. At lower frequency, the SIW cavity's second mode (TE_{120}) excites the slot. By contrast, the slot is also excited at higher frequency in the modified-TE_{120} mode. The polarization-flexible characteristic is obtained by using two different inputs that generate two orthogonal linearly polarized beams. Hence, the proposed antenna can provide freedom to choose any polarization states at two target frequencies. It is noted that there have been dual-band and dual-polarized SIW cavity antennas reported previously, but they have not provided full control of polarization status [7]. This letter is organized as follows. The proposed antenna structure and the operating concept are explained in Section II. In Section III, the simulated and measured results of the proposed antenna are provided.

II. Antenna Structure and Operation

The square cavity with a square or circular slot can provide single-band broadside radiation [8]. For dual-band broadside radiation, conductor strips should be located at the centers of the square slot's four sides. Fig. 1 shows the proposed dual-band and polarization-flexible cavity antenna and its dimensions. The polarization-agile characteristic is realized by two orthogonal feeding lines.

A. Dual-Band Operation

The z-directed electric field distributions in the first patch mode and the second patch mode are shown in Fig. 2(a) and (b), respectively. In the first patch mode, the SIW cavity is excited by the TE_{120} ($\mathrm{TE}_{\mathrm{xyz}}$) mode, and it builds a TM_{010} mode

Manuscript received April 30, 2015; revised June 24, 2015; accepted July 01, 2015. Date of publication July 08, 2015; date of current version March 02, 2016. This work was supported in part by Tubistech Corporation and Hybrid Quantum Corporation.

H. Lee and T. Itoh are with the Electrical Engineering Department, University of California, Los Angeles, Los Angeles, CA 90095 USA (e-mail: ucla.hlee@gmail.com; itoh@seas.ucla.edu).

Y. Sung is with the Department of Electronic Engineering, Kyonggi University, Suwon 443-760, Korea (e-mail: yjsung@kyonggi.ac.kr).

C.-T. M. Wu is with the Department of Electrical and Computer Engineering, Wayne State University, Detroit, MI 48202, USA (e-mail: ctmwu@wayne.edu).

Color versions of one or more of the figures in this paper are available online at http://ieeexplore.ieee.org.

Digital Object Identifier 10.1109/LAWP.2015.2453993

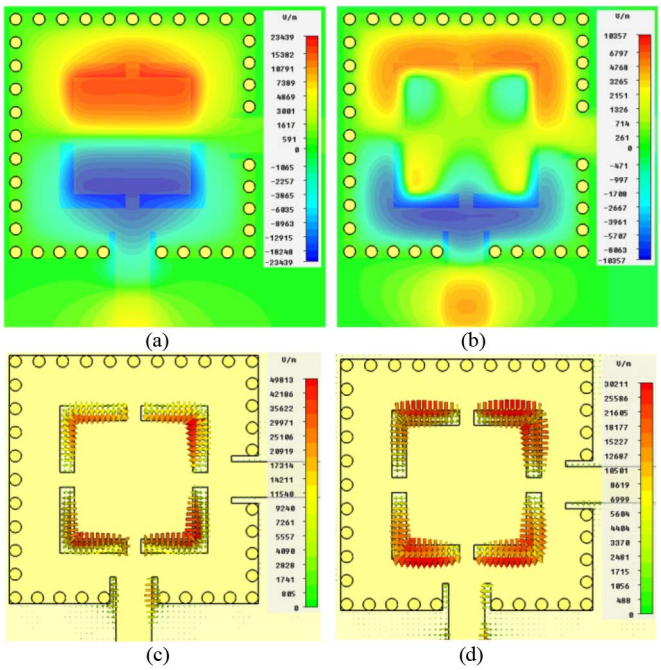

Fig. 2. z-directed electric field distributions inside the cavity (port 1 excitation and port 2 terminated by 50 Ω): (a) first patch mode and (b) second patch mode. Tangential electric field distribution on the slot: (c) first patch mode and (d) second patch mode.

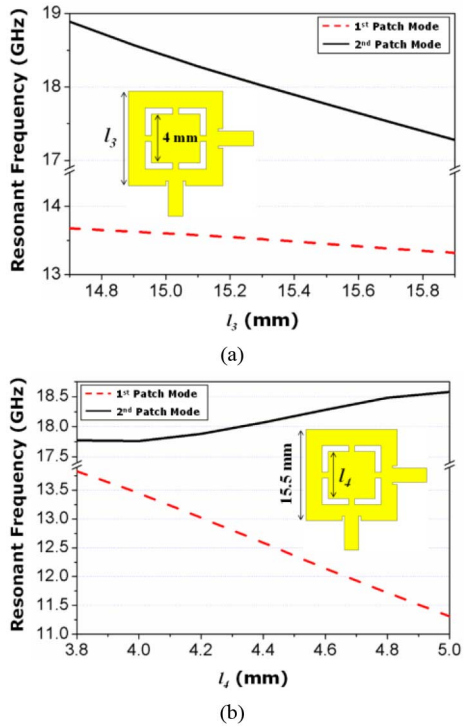

Fig. 3. Change of two resonant frequencies versus (a) the rectangular cavity length (l_3) and (b) the inner rectangular patch length (l_4).

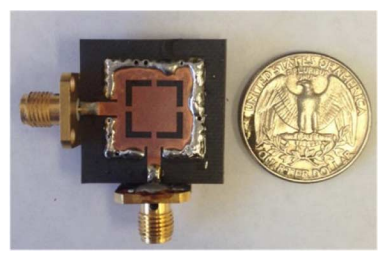

Fig. 4. Photograph of the proposed antenna.

for the inner patch [9]. By contrast, the second broadside radiation is generated by an unconventional mode. This mode works similarly to the conventional TE_{120} mode. However, because of the perturbation from the slot and the inner patch, the effective cavity length in the y-direction becomes smaller than the original cavity length. The conductor strips located at the four sides of the slot help to generate this mode. Fig. 2(c) and (d) shows the tangential electric fields on the slots at lower and higher frequencies, respectively. In both patch modes, only y-directed electric fields contribute radiation. Meanwhile, x-directed electric fields cancel each other out.

Changes in the two resonant frequencies versus the rectangular cavity length l_3 are shown in Fig. 3(a). For the simplicity, conductive walls are used instead of via walls in simulation. Other dimensions are the same as those of the antenna shown in Fig. 1. As cavity length l_3 increases, both resonant frequencies decrease. This result is consistent with the explanation that the TE_{120} and modified-TE_{120} modes excite the cavity at two resonant frequencies. In addition, it is worth noting that the change of the first resonant frequency is slower than that of the second resonant frequency because the length of the inner patch side is fixed at 4 mm. Fig. 3(b) shows the change in the two resonant frequencies versus the inner rectangular patch length l_4. We can observe that increasing length l_4 significantly lowers the resonant frequency of the first patch mode. This is because the inner patch, whose size has increased, is excited by the TM_{010} mode at a lower frequency. By contrast, in the second patch mode, a larger value of l_4 increases the resonant frequency. This occurs because the increased inner patch reduces the effective outer cavity length in the y-direction, thereby increasing the resonant frequency of the second patch mode. Two operating bands can be controlled by adjusting a cavity size and slot dimensions for diverse applications. The frequency range shown in Fig. 3 can be used for several Ku-band satellite applications such as broadcasting satellite systems and fixed satellite systems.

B. Polarization-Flexibility

Table I shows the possible polarization states of the proposed antenna. In the third column of the table, a solid black arrow indicates the E-field direction excited by port 1, and a dotted red arrow indicates the E-field direction excited by port 2. A green arrow represents the sum of the two E-fields from ports 1 and 2. With six excitation combinations, six major polarization states can be implemented by the proposed antenna.

III. Simulated and Measured Results

Fig. 4 is a photograph of the fabricated antenna. The prototype of the antenna uses an RT/duroid 5880 substrate ($\varepsilon_r = 2.2$, $h = 1.575$ mm). Via holes with a diameter of $d = 0.8$ mm are placed on each side of the SIW cavity to emulate conductive walls. To ensure good electrical contact, the vias and both top and bottom sides are soldered. In terms of free-space

TABLE I
POSSIBLE POLARIZATION STATES

Polarization Status	Ports Excited Signal	E-Field on Slots
Linear Polarization along Y-direction	$A_1 \neq 0$ and $A_2 = 0$	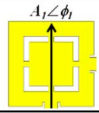
Linear Polarization along X-direction	$A_1 = 0$ and $A_2 \neq 0$	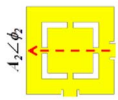
Linear Polarization along $\phi = +45°$	$A_1 = A_2$ & $\lvert\phi_1 - \phi_2\rvert = 180°$	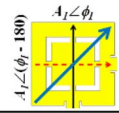
Linear Polarization along $\phi = +135°$	$A_1 = A_2$ & $\phi_1 = \phi_2$	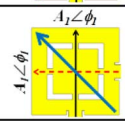
Left-Handed Circular Polarization (LHCP)	$A_1 = A_2$ & $\phi_1 - \phi_2 = -90°$	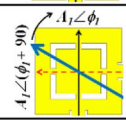
Right-Handed Circular Polarization (RHCP)	$A_1 = A_2$ & $\phi_1 - \phi_2 = +90°$	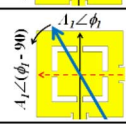

Port 1 signal magnitude: A_1, Port 1 signal phase: ϕ_1, Port 2 signal magnitude: A_2, Port 2 signal phase: ϕ_2

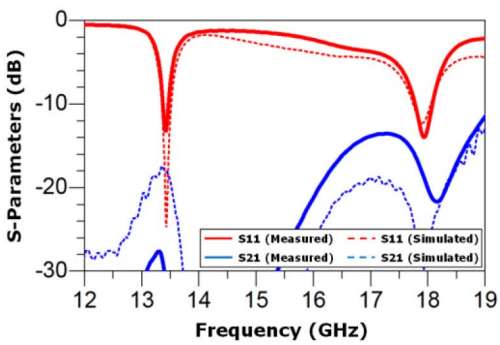

Fig. 5. S-parameters of the proposed antenna.

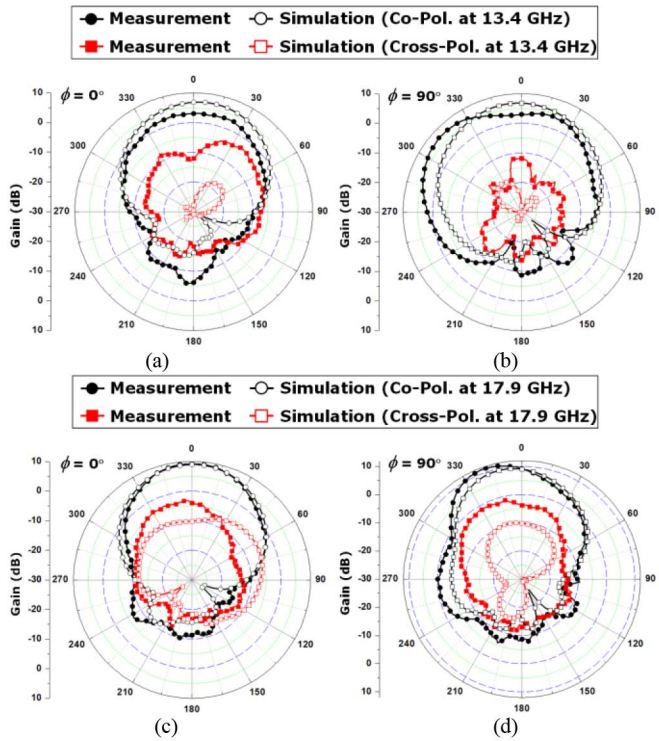

Fig. 6. Gain patterns of the first patch mode at (a) xz-plane and (b) yz-plane. Gain patterns of the second patch mode at (c) xz-plane and (d) yz-plane.

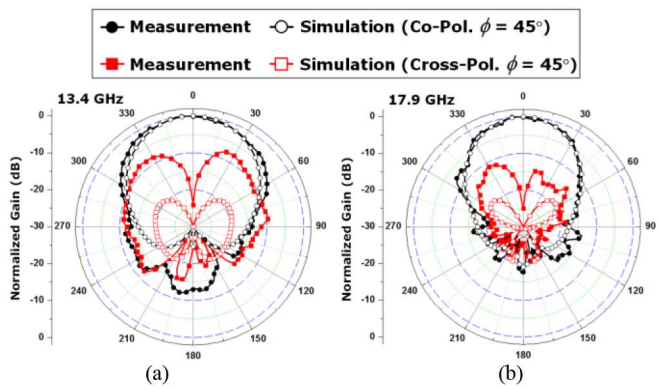

Fig. 7. Normalized gain patterns of (a) the first patch mode and (b) the second patch mode at $\phi = 45°$ plane.

wavelength (λ_0), the antenna cavity size is $0.75\lambda_0 \times 0.75\lambda_0$ at 13.4 GHz and $1\lambda_0 \times 1\lambda_0$ at 17.9 GHz. The simulated and measured S-parameters of the proposed antenna are shown in Fig. 5. In the first patch mode (at 13.4 GHz), the measured return loss is larger than 13.4 dB, and the measured isolation between the two ports is greater than 31 dB. The second patch mode operates at 17.9 GHz. At the second resonant frequency, the measured S_{11} is -14 dB, and the measured S_{21} is -19 dB. With 10-dB return loss criterion, the proposed antenna shows 150 MHz (fractional bandwidth (Δ) : 1.1%) and 350 MHz (Δ : 2.0%) bandwidths in the first mode and the second mode, respectively. Overall, the measured S-parameters show strong agreement with the simulated results.

To verify the concept of the proposed antenna, far-field patterns with various polarization states are measured. y-directed linear polarization and linear polarization along $\phi = 135°$ are measured in the far-field chamber. The near-field chamber is used to measure the (left-hand circularly polarized) LHCP state. Fig. 6 shows the far-field patterns with y-directed linear polarization. As expected, the proposed antenna shows broadside radiation patterns at both targeted frequencies. It is worth noting that, because of the larger effective aperture size, the antenna gain at 17.9 GHz is higher than at 13.4 GHz. The measured cross-polarization levels at both frequencies are approximately 15 dB less than the copolarization levels on the boresight.

The far-field patterns with linear polarization along $\phi = 135°$ are shown in Fig. 7. Since it is difficult to measure a direct beam pattern with linear polarization along $\phi = 135°$ in our chamber, the antenna under test (AUT) is rotated 45°

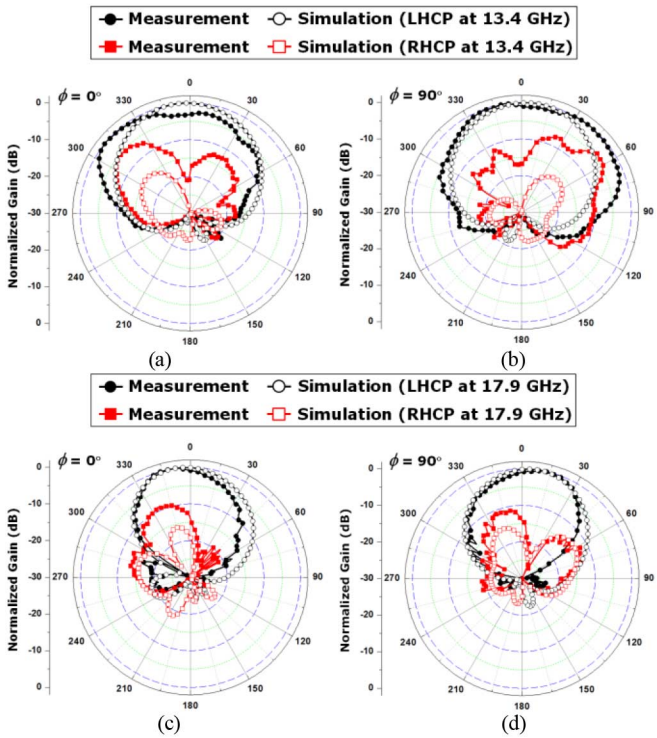

Fig. 8. Normalized gain patterns of the first patch mode at (a) xz-plane and (b) xy-plane. Gain patterns of the second patch mode at (c) xz-plane and (d) yz-plane.

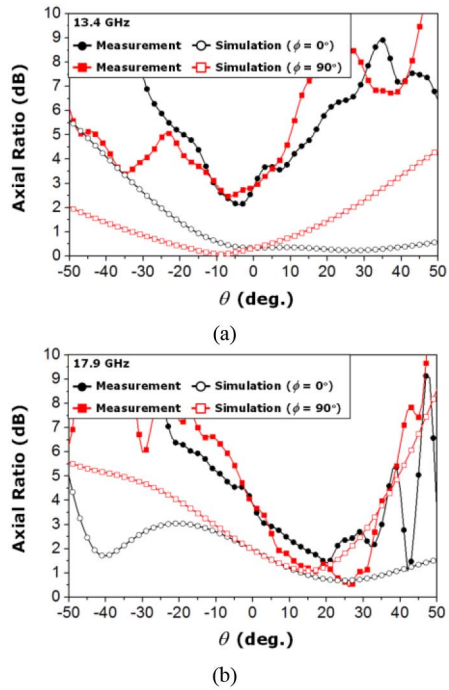

Fig. 9. Axial ratio of (a) the first patch mode and (b) the second patch mode.

along the z-axis and measured, thereby providing far-field patterns with a $\phi = 45°$ cut. For this measurement, a broadband power divider manufactured by the Narda Corporation is used. In Fig. 7, we can observe measured cross-polarization levels that are approximately 25 dB less than the copolarization levels on the boresight. LHCP beam patterns from the proposed antenna are shown in Fig. 8. The commercial broadband 90° coupler (Narda Corporation) is connected to the proposed antenna for generating a CP beam. The measured cross-polarization levels at both frequencies are approximately 15 dB less than the copolarization levels on the boresight. Axial ratio (AR) of the antenna with CP configuration is also provided in Fig. 9. With 3-dB AR criterion, the proposed antenna shows 600 MHz ($\Delta : 4.5\%$) and 300 MHz ($\Delta : 1.7\%$) AR bandwidth in the first mode and the second mode, respectively. Because of the symmetry, we can expect similar results in the other three polarization states [x-directed, along $\phi = 45°$, and right-hand circularly polarized (RHCP)]. Overall, the measured results are consistent with the simulated results. However, the measured cross-polarization levels are higher than the simulated results. This may be the result of imperfect cancelation of the x-directed tangential electric field (with port 1 excitation) or the y-directed tangential electric field (with port 2 excitation) on the slot. In addition, scatterings from the SMA connectors and additional components (the power divider and the coupler) could affect the cross-polarization levels. The measured AR degradation observed in Fig. 9 may also be resulted from same reasons including the asymmetry cavity shape and the discontinuities on the cavity wall.

IV. Conclusion

A novel dual-band and polarization-flexible SIW cavity antenna is presented. Through a modified square slot, the proposed cavity structure has two resonances that generate broadside radiation patterns. The resonant frequencies can be controlled by changing the cavity size and the slot size. Moreover, the proposed antenna has two orthogonal feeding lines with strong isolation at two resonant frequencies. This generates various polarized beams. With these advantages, we expect the proposed antenna to be beneficial for various communication systems that require a dual band and polarization diversity.

References

[1] S. Chen, D. Dong, Z. Liao, Q. Cai, and G. Liu, "Compact wideband and dual-band antenna for TD-LTE and WLAN applications," *Electron. Lett.*, vol. 50, pp. 1111–1112, Jul. 2014.

[2] S. H. S. Esfahlani, A. Tavakoli, and P. Dehkhoda, "A compact single-layer dual-band microstrip antenna for satellite applications," *IEEE Antennas Wireless Propag. Lett.*, vol. 10, pp. 931–934, 2011.

[3] S. Gao, A. Sambell, and S. S. Zhong, "Polarization-agile antennas," *IEEE Antennas Propag. Mag.*, vol. 48, pp. 28–37, Jun. 2006.

[4] Y. Sung, T. Jang, and Y. Kim, "A reconfigurable microstrip antenna for switchable polarization," *IEEE Microw. Wireless Compon. Letters*, vol. 14, no. 11, pp. 534–536, Nov. 2004.

[5] P. Qin, Y. J. Guo, and C. Ding, "A dual-band polarization reconfigurable antenna for WLAN systems," *IEEE Trans. Antennas Propag.*, vol. 61, no. 11, pp. 5706–5713, Nov. 2013.

[6] H. Moghadas, M. Daneshmand, and P. Mousavi, "A dual-band high-gain resonant cavity antenna with orthogonal polarization," *IEEE Antennas Wireless Propag. Lett.*, vol. 10, pp. 1220–1223, 2011.

[7] G. Q. Luo, Z. F. Hu, Y. Liang, L. Y. Yu, and L. L. Sun, "Development of low profile cavity backed crossed slot antenna for planar integration," *IEEE Trans. Antennas Propag.*, vol. 57, no. 10, pp. 2972–2979, Oct. 2009.

[8] C. M. Wu, J. H. Choi, H. Lee, and T. Itoh, "Magnetic-current-loop induced electric dipole antenna based on substrate integrated waveguide cavity," *IEEE Antennas Wireless Propag. Lett.*, vol. 13, pp. 519–522, Mar. 2014.

[9] C. Balanis, "Microstrip antennas," in *Antenna theory: Analysis and design*. New York, NY, USA: Wiley, 2005.